3392–3402 *Nucleic Acids Research, 2012, Vol. 40, No. 8* *Published online 30 December 2011*
doi:10.1093/nar/gkr1273

Transcription initiation factor DksA has diverse effects on RNA chain elongation

Ran Furman, Anastasiya Sevostyanova and Irina Artsimovitch*

Department of Microbiology and The Center for RNA Biology, Ohio State University, Columbus, OH 43210, USA

Received November 8, 2011; Revised December 7, 2011; Accepted December 8, 2011

ABSTRACT

Bacterial transcription factors DksA and GreB belong to a family of coiled-coil proteins that bind within the secondary channel of RNA polymerase (RNAP). These proteins display structural homology but play different regulatory roles. DksA disrupts RNAP interactions with promoter DNA and inhibits formation of initiation complexes, sensitizing rRNA synthesis to changes in concentrations of ppGpp and NTPs. Gre proteins remodel the RNAP active site and facilitate cleavage of the nascent RNA in elongation complexes. However, DksA and GreB were shown to have overlapping effects during initiation, and *in vivo* studies suggested that DksA may also function at post-initiation steps. Here we show that DksA has many features of an elongation factor: it inhibits both RNA chain extension and RNA shortening by exonucleolytic cleavage or pyrophosphorolysis and increases intrinsic termination *in vitro* and *in vivo*. However, DksA has no effect on Rho- or Mfd-mediated RNA release or nascent RNA cleavage in backtracked complexes, the regulatory target of Gre factors. Our results reveal that DksA effects on elongating RNAP are very different from those of GreB, suggesting that these regulators recognize distinct states of the transcription complex.

INTRODUCTION

Transcription factor DksA acts synergistically with an alarmone ppGpp to control the bacterial response to stress and starvation (1,2). DksA belongs to a class of bacterial regulators (which includes GreA, GreB and Gfh1) that do not interact with the nucleic acids and instead directly bind in the RNA polymerase (RNAP) secondary channel, which connects the active site to the surface and serves as a conduit for the substrate NTPs. These regulators have no sequence similarity but possess a common structural organization (Supplementary Figure S1): they are entirely helical and composed of a coiled-coil (CC) domain and a globular domain. The CC domains that are similar among these proteins extend through the secondary channel toward the RNAP active site, whereas the structurally different globular domains bind outside of the channel. The residues at the CC tip of these proteins approach the RNAP active site enabling their defined regulatory functions (3–5).

GreB enhances hydrolytic cleavage of the backtracked RNA in arrested transcription elongation complexes (ECs), restoring productive transcription (3). GreB is thought to deliver the low-affinity catalytic Mg^{2+} ion bound to two carboxylates at the end of its CC to the RNAP active site that contains the primary, high-affinity Mg^{2+} ion, thereby completing the Mg^{2+} catalytic pair (6). Gfh1 has four acidic residues at the CC tip and inhibits catalysis by blocking the substrate NTP binding and stabilizing an inactive RNAP conformation (5). DksA exerts its major documented effect before catalysis, by binding to some promoter complexes and altering the transcription initiation pathway (7,8). On the other hand, the proximity of the DksA CC tip to the RNAP active site suggests additional effects on catalysis.

In this work, we analyzed *Escherichia coli* DksA effects on post-initiation activities of RNAP. We show that DksA inhibits transcript elongation, exonucleolytic RNA cleavage and pyrophosphorolysis in a purified *in vitro* system. DksA also increases factor-independent termination *in vivo* and *in vitro*. These activities are enhanced by ppGpp and by a 'gain-of-function' substitution in DksA (9). The effects of DksA on elongation are quite distinct from those of GreB, even though we show that the two proteins likely recognize the same region on the RNAP β′ subunit. These observations suggest that DksA and GreB bind to different states of the EC.

MATERIALS AND METHODS

Proteins and reagents

Oligonucleotides were obtained from Integrated DNA Technologies (Coralville, IA, USA), NTPs, from GE

*To whom correspondence should be addressed. Tel: +1 614 292 6777; Fax: +1 614 292 8120; Email: artsimovitch.1@osu.edu
Present address:
Anastasiya Sevostyanova, Section of Microbial Pathogenesis, Yale School of Medicine, New Haven, CT, 06536, USA.

Healthcare (Piscataway, NJ, USA), [α^{32}P]-NTPs and [γ^{32}P]-ATP, from Perkin Elmer (Waltham, MA, USA), restriction and modification enzymes, from NEB (Ipswich, MA, USA), polymerase chain reaction (PCR) reagents, from Roche (Indianapolis, IN, USA), other chemicals, from Sigma (St. Louis, MO, USA) and Fisher (Pittsburgh, PA, USA). ppGpp was from TriLink BioTech (San Diego, CA, USA). Plasmid DNAs and PCR products were purified using kits from Qiagen (Valencia, CA, USA) and Promega (Madison, WI, USA). All plasmids are listed in the Supplementary Table S1. DksA (4), Mfd (10) and RNAP (11) were purified as described previously. Rho protein was a gift from Jeff Roberts. DksA^{A35C} was labeled with Alexa Fluor 546 maleimide (Invitrogen, Carlsbad, CA, USA); an excess dye was removed using G50 columns (GE Health). Labeling efficiency ranged between 60 and 100%. Labeling did not affect DksA activity.

In vitro RNA synthesis

Templates for *in vitro* transcription were generated by PCR amplification. For inhibition assays, linear pIA171 DNA template (40 nM), RNAP holoenzyme (50 nM), and substrates (150 μM ApU, 5 μM ATP and GTP, 2 μM CTP, 2 μCi of [α^{32}P]-CTP; 3000 Ci/mmol) were incubated with DksA in TGA2 buffer (20 mM Tris-acetate, 20 mM Na acetate, 2 mM Mg acetate, 14 mM 2-mercaptoethanol, 0.1 mM EDTA, 5% glycerol, pH 7.9) for 15 min at 37°C. For elongation and intrinsic termination assays, halted ECs were formed on templates indicated in figure legends in TGA2 with the starting substrates (150 μM ApU, 5 μM ATP and GTP, 2 μM CTP, 2 μCi of [α^{32}P]-CTP; 3000 Ci/mmol); elongation was carried out as described in figure legends. The reactions were quenched by addition of an equal volume of STOP buffer (10 M urea, 50 mM EDTA, 45 mM Tris-borate; pH 8.3, 0.1% bromophenol blue, 0.1% xylene cyanol).

RNA cleavage assays

Halted complexes (A26) were prepared on pIA226 template in TGA2 buffer supplemented with ApU at 150 μM, ATP and UTP at 2.5 μM, GTP at 1 μM, and 5 μCi of [α^{32}P]GTP (3000 Ci/mmol) during 15 min incubation at 37°C and purified through G50 spin columns (GE Health). For endonucleolytic cleavage, DksA and ppGpp (or storage buffer and water) were added to A26 complexes at 37°C. For exonucleolytic cleavage, halted unlabeled A26 ECs (100 nM) were incubated with ^{32}P-[αCTP] to generate 3′-labeled C27 nascent RNA, as described in (12). DksA and ppGpp were incubated with C27 ECs for 3 min at 37°C, followed by addition of 10 mM $MnCl_2$. Reactions were quenched with the STOP buffer at selected times, and loaded onto 10% gels.

DNaseI footprinting

C147 ECs were formed on pRL596 PCR fragment ([γ^{32}P]-labeled on the template strand, at 20 nM), WT holo RNAP (400 nM), 25 μM ATP, GTP, CTP and 100 μM ApU in 44 mM Tris–HCl, 14 mM $MgCl_2$, 20 mM NaCl, 5% glycerol, 0.1 mM EDTA, pH 7.9. DksA^{N88I} and ppGpp were added to 2 μM and 100 μM where indicated. After 2 min of incubation, the complexes were treated with 0.15 U of DNaseI (Epicentre, Madison, WI, USA) for 1 min and quenched by the addition of an equal volume of phenol. Samples were subjected to phenol–chloroform extraction, precipitated with ethanol, and dissolved in 96% formamide.

Sample analysis

Samples were heated for 2 min at 90°C and separated by electrophoresis in denaturing acrylamide (19:1) gels (7 M Urea, 0.5X TBE) of various concentrations (5–10%). RNA products were visualized and quantified using a PhosphorImager Storm 820 System (GE Healthcare), ImageQuant Software, and Microsoft Excel.

Binding assays

Steady-state fluorescence anisotropy experiments were performed using F-7000 spectrophotometer (Hitachi). The excitation wavelength was 555 nm and polarization was detected at 571 nm, G value was determined prior to each experiment. DksA (5–20 nM) was mixed with increasing concentrations of RNAP at 30°C in 20 mM HEPES, pH 7.5, 50 mM NaCl and 1 mM β-mercaptoethanol. The system reached steady state after 10 min. The data were analyzed using Scientist software (Micromath). Fe cleavage assays were performed as described in (13) using Alexa 546 - labeled DksA^{A35C}. Gels were analyzed using Typhoon 900 (GE Healthcare); see also Supplementary Data.

RESULTS

DksA and GreB may use the same target on the RNAP surface

Structural and biochemical data reveal that a coiled-coil domain in the β′ subunit (β′ rim helices; β′RH, residues 649–717), which forms the rim of the secondary channel, serves as a binding site for GreB and Gfh1. Despite their dramatically different effects on RNAP, GreB and Gfh1 are proposed to utilize the same mode of interactions (Figure 1A) between the tip of the β′RH and a hydrophobic region on the globular domain of the regulators (3,5,11). Moreover, GreB can functionally substitute for DksA during initiation (14), suggesting that DksA may also bind to RNAP similarly. In contrast, in an earlier model of RNAP/DksA/ppGpp (4), the RH tip does not make any contacts to DksA (Figure 1A). Importantly, this model was built by rigid-body docking of the *E. coli* DksA onto *Thermus thermophilus* RNAP using a hypothesis that RH-DksA contacts are similar to DksA–DksA crystal packing contacts observed in the *E. coli* DksA structure.

To determine whether DksA and GreB use similar determinants on RNAP, we tested effects on DksA activity of changes in RNAP that were previously demonstrated to confer resistance to GreB (11). We used the enzyme lacking the β′i6 (also called β′SI3 (15); β′residues 943–1130), a large domain inserted into the mobile β′trigger loop (TL; β′residues 926–942 and 1131–1146)

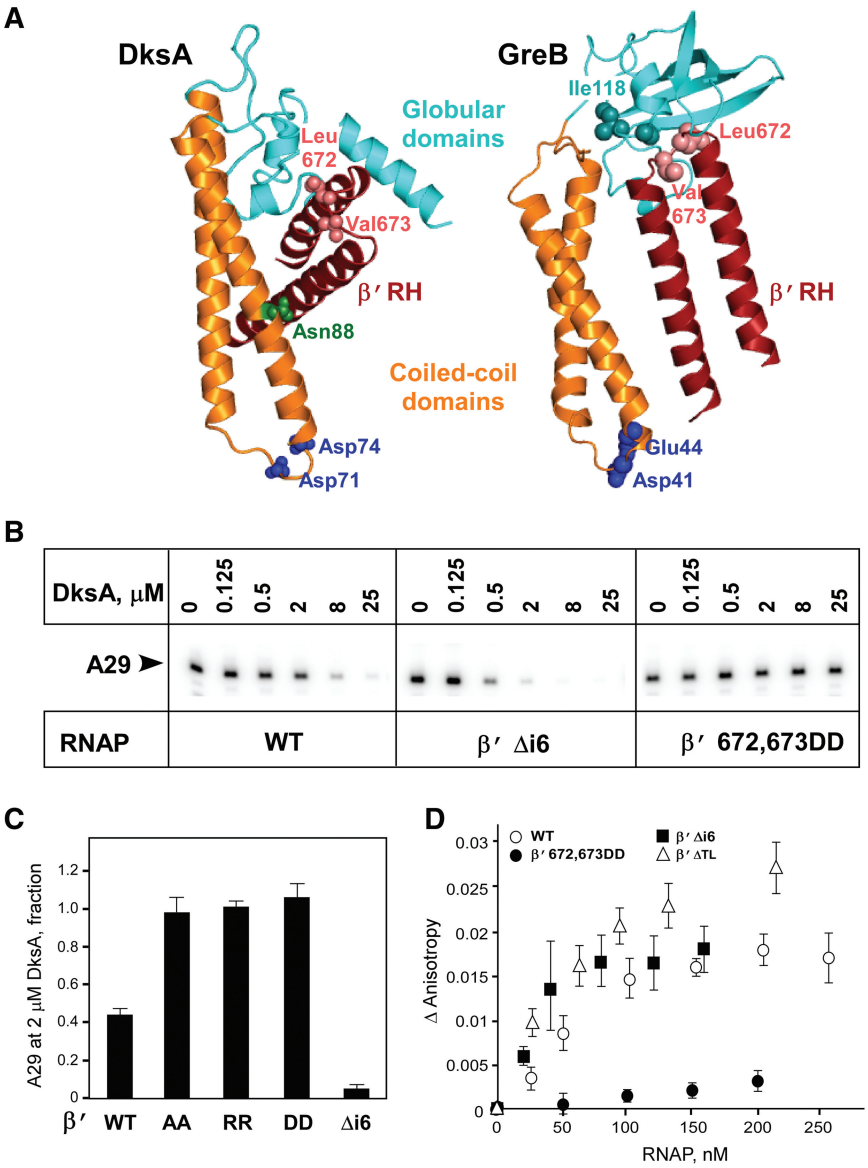

Figure 1. DksA binds to the β′ RH. (**A**) Proposed interactions of DksA (4) and GreB (11) with the β′RH. The CC domains (orange) of DksA (left) and GreB (right) carry the functionally important acidic residues (blue spheres) at their tips. The globular domains (cyan) interact with the β′RH (dark red). The β′RH residues Leu672 and Val673 are shown as salmon spheres, the GreB residues required for binding to RNAP, as cyan spheres. The side chain of DksA Asn88 is colored green. (**B**) Inhibition of radiolabeled A29 RNA synthesis by DksA^{WT} on pIA171 template; DksA was added at indicated concentrations during initiation. A representative gel is shown. (**C**) Inhibition of A29 RNA synthesis measured for different RNAPs at 2 μM DksA; the data are presented as average of three independent experiments ± standard deviation and were normalized relative to the amount of A29 RNA synthesized in the absence of DksA. (**D**) DksA binding to the WT, β′RH^{DD}, β′Δi6 and β′ΔTL enzymes assayed by fluorescence polarization; the results of three independent experiments are shown. $K_{D,app}$ were 102 ± 13 nM for WT, 42 ± 7 nM for β′Δi6, and 80 ± 5 nM for the β′ΔTL RNAP; $K_{D,app}$ for the β′RH^{DD} could not be determined.

and located near the entrance into the secondary channel (16), and RNAPs with substitutions at the tip of the RH.

We previously showed that double substitutions of the *E. coli* RH residues β′Leu672 and Val673 for Ala or Asp reduced or abolished, respectively, GreB enhancement of RNA cleavage and binding to RNAP (11). We tested the effects of these substitutions on inhibition of RNA synthesis from the T7A1 promoter by DksA (Figure 1B). We monitored the formation of radiolabeled A29 RNA on pIA171 template at increasing concentrations of DksA as described previously (4). We found that the Ala substitutions of β′Leu672 and Val673 strongly reduced inhibition by DksA as compared to the wild-type (WT) RNAP, and substitutions for charged residues completely abolished it. On the other hand, the deletion of the i6, which makes RNAP insensitive to GreB (17), strongly enhanced the inhibitory effect of DksA (Figure 1C).

To test whether the lack of DksA effect on enzymes with RH substitutions was due to the loss of DksA binding to RNAP, we carried out Fe-mediated cleavage (Supplementary Figure S2) and fluorescence anisotropy assays (Figure 1D). Both assays revealed that the double

Asp substitution (RH^{DD}) dramatically reduced DksA binding to core RNAP, consistent with a loss of DksA-RH contacts at the mutation site or a loss of interactions due to a different conformation of the altered RH. These findings support a model in which the RH domain interacts with both GreB and DksA, resulting in partially overlapping effects of these factors on transcription initiation (14).

The i6 deletion increased the affinity of DksA for the core RNAP by more than 2-fold (K_d = 42 nM compared to 97 nM for the WT RNAP; Figure 1D), whereas the deletion of the entire TL-i6 region had a smaller effect (K_d = 80 nM). Consistent with the report from the Gourse lab (8), our results show that the TL is dispensable for DksA binding. The stimulatory effect of Δi6 suggests that the i6 domain interferes with DksA binding directly or indirectly, by favoring a TL state that is incompatible with DksA binding.

DksA alters RNA chain elongation *in vitro* in synergy with ppGpp

Chamberlin and coauthors showed that ppGpp inhibits RNA synthesis on phage T7 DNA (18). The action of ppGpp is not competitive with NTP substrates and is exerted at specific sites along the template; similar effects were observed on other templates (19,20). Given that ppGpp and DksA generally (but not always) act synergistically, we tested if *E. coli* DksA also affects elongation. We compared the effects of the WT DksA and its hyperactive variant with a substitution of Asn88 for Ile ($DksA^{N88I}$), which has been reported to increase DksA affinity for RNAP and reduce DksA dependence on ppGpp (9). In our experiments, we used physiological concentrations of DksA (14) and ppGpp (21).

Both DksA variants inhibited transcription from a T7A1 promoter (Supplementary Figure S3), which forms relatively unstable open complexes. The effect of $DksA^{WT}$ was modest and was strongly enhanced by ppGpp. In contrast, $DksA^{N88I}$ almost completely abolished RNA synthesis even at very low ppGpp. In these reactions, DksA was added prior to NTPs and could exert its effect either before or during catalysis.

We next tested the effects of DksA on elongation by adding this factor to preformed halted ECs. We carried out a standard single-round transcription assay using a linear pIA146 template with a T7A1 promoter followed by *E. coli rpoB* gene, which is devoid of strong pause signals. On this template, a radiolabeled ECs is stalled after incorporation of an A residue at position 29 when transcription is initiated in the absence of UTP. RNAP resumes elongation upon the addition of all NTP substrates and heparin (to prevent re-initiation); the rate of RNAP progression is monitored by withdrawing aliquots from the reaction mixture at given times.

With the WT RNAP (Figure 2A), DksA variants at 2 μM had no (WT) or a small (1.2-fold for N88I) inhibitory effect on an apparent rate of RNA chain extension. ppGpp (at 30 μM) had a 1.4-fold effect and acted synergistically with DksA (particularly $DksA^{N88I}$, 6.3-fold combined effect) to slow the enzyme down (Figure 2A). The effect of DksA alone was increased at higher concentrations (Supplementary Figure S4). In this and other experiments we find that the effect of the N88I substitution can be matched by an increase in concentration of $DksA^{WT}$, consistent with an increased affinity of $DksA^{N88I}$ for RNAP (9) being the sole reason for this effect. Since the cellular level of DksA is quite high [5 μM; (14)], in our work we use $DksA^{N88I}$ in place of $DksA^{WT}$ to increase the occupancy of RNAP by DksA at lower protein concentrations. The DksA effects on elongation were augmented by the i6 deletion; ppGpp and $DksA^{N88I}$ together slowed this enzyme down 40-fold (Figure 2B). ppGpp and DksA also inhibited pyrophosphorolysis, the reversal of the nucleotide addition reaction (Supplementary Figure S5).

DksA increases intrinsic transcription termination *in vitro* and *in vivo*

We reported that ppGpp increases the efficiency of the *rrnB* T1 terminator during *in vitro* transcription by *E. coli* RNAP (19). Since DksA and ppGpp often have similar effects on transcription, we wanted to test whether DksA can also increase termination. We constructed a template which encodes a 105-nt G-less initial transcribed region followed by a minimal *rrnB* T1 signal. On this template, termination efficiency at *rrnB* T1 can be reduced by a combination of the initial transcribed sequence and high concentrations of Mg^{2+}, allowing us to measure the stimulatory effects of DksA and ppGpp. We found that $DksA^{N88I}$ (at 2 μM) increased WT RNAP termination at *rrnB* T1 ~2.4-fold (Figure 3A); the same effect was observed with $DksA^{WT}$ at 5 μM (not shown). ppGpp modestly enhanced termination both in the absence and in the presence of $DksA^{N88I}$. DksA also increased termination on a template encoding *rrnB* T1 in its natural context (Supplementary Figure S6) and at a phage λ tr2 terminator (Supplementary Figure S7). The Δi6 enzyme terminated with lower efficiency, as expected from a 'fast' RNAP (15); the addition of $DksA^{N88I}$ increased *rrnB* T1 efficiency more than 7-fold in the absence of ppGpp and essentially abrogated readthrough in the presence of ppGpp. By contrast, the $\beta'RH^{DD}$ RNAP failed to respond to DksA either in the absence or in the presence of ppGpp. The DksA effect was comparable to that of general elongation factor NusA (Figure 3B). These results demonstrate that DksA increases termination *in vitro*.

To assess whether DksA may increase termination *in vivo*, we constructed two reporter plasmids that encode *Photorhabdus luminescens luxCDABE* operon under control of T7A1 promoter, with and without *rrnB* T1 positioned between the promoter and the *lux* genes. We found that *rrnB* T1 reduced *lux* expression ~28-fold in a wild-type *dksA* strain and ~9.6-fold in a Δ*dksA* strain (Figure 3C). This result is consistent with the direct DksA effect on termination under normal *E. coli* growth conditions. In these assays, we also observed a 1.4-fold inhibitory effect of DksA at the T7A1 promoter *in vivo*, which is consistent with our observations *in vitro* (Figure 1B).

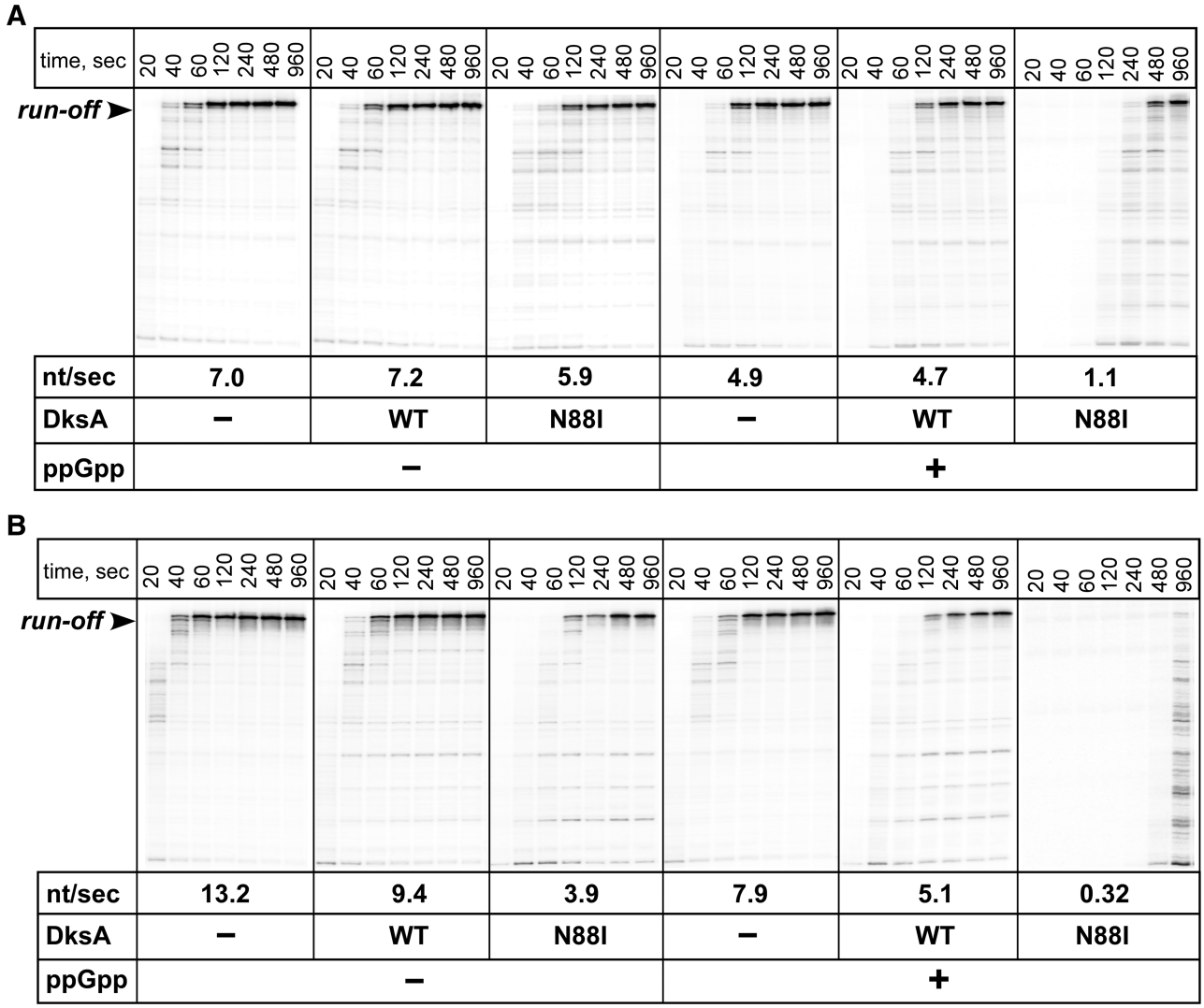

Figure 2. DksA and ppGpp decrease an apparent rate of RNA chain elongation. Single-round elongation assays on pIA146 template encoding a pause-less *rpoB* region with the WT (**A**) and β′Δi6 (**B**) RNAPs. Halted radiolabeled A29 ECs (40 nM) were incubated with DksA (WT or N88I, at 2 μM) and ppGpp (30 μM), where indicated, for 3 min at 37°C. Elongation was restarted by the addition of 250 μM NTPs and 10 μg/ml heparin. Aliquots were quenched at the selected times and analyzed on 5% denaturing gels. Representative gels with a region near the run-off RNA (661 nt) are shown. The assay was repeated at least three times for each combination of factors; the differences between independent measurements were within 10%.

DksA does not affect Rho-dependent termination *in vitro*

We next tested whether DksA alters the activity of the termination factor Rho on a pIA267 template (Figure 4) encoding a phage λ tR1 Rho-dependent termination signal (22). In the absence of DksA, most RNAP molecules reached the end of the linear DNA template, forming run-off transcripts. Addition of Rho (to 25 nM to induce partial release) caused termination at multiple sites, thereby reducing the run-off product more than 2-fold. Although $DksA^{WT}$ and $DksA^{N88I}$ induced RNAP pausing/arrest at some sites, particularly in the presence of ppGpp, the overall efficiency of Rho-dependent termination and the pattern of release products did not change dramatically when either DksA variant was also present, with or without ppGpp. We conclude that neither DksA nor ppGpp alter Rho activity, at least *in vitro*.

DksA effects on RNA cleavage in stalled ECs

The secondary channel regulators are known to affect cleavage of the nascent RNA by RNAP. Gfh1 strongly inhibits both exo- and endonucleolytic cleavage reactions (23), whereas Gre factors strongly stimulate the endonucleolytic reaction to rescue arrested ECs (3). To determine whether DksA alters the nascent RNA cleavage, we used the ECs that are susceptible to cleavage.

First, we tested the effect on exonuclease activity. We formed unlabeled A26 TECs on a λP_R template pIA226, removed NTPs by gel filtration, and extended the nascent RNA by addition of [α-^{32}P]CMP. The 3′-labeled C27 ECs were used to monitor the release of the labeled CMP that occurred upon exonucleolytic cleavage (Figure 5A). When C27 ECs were incubated at

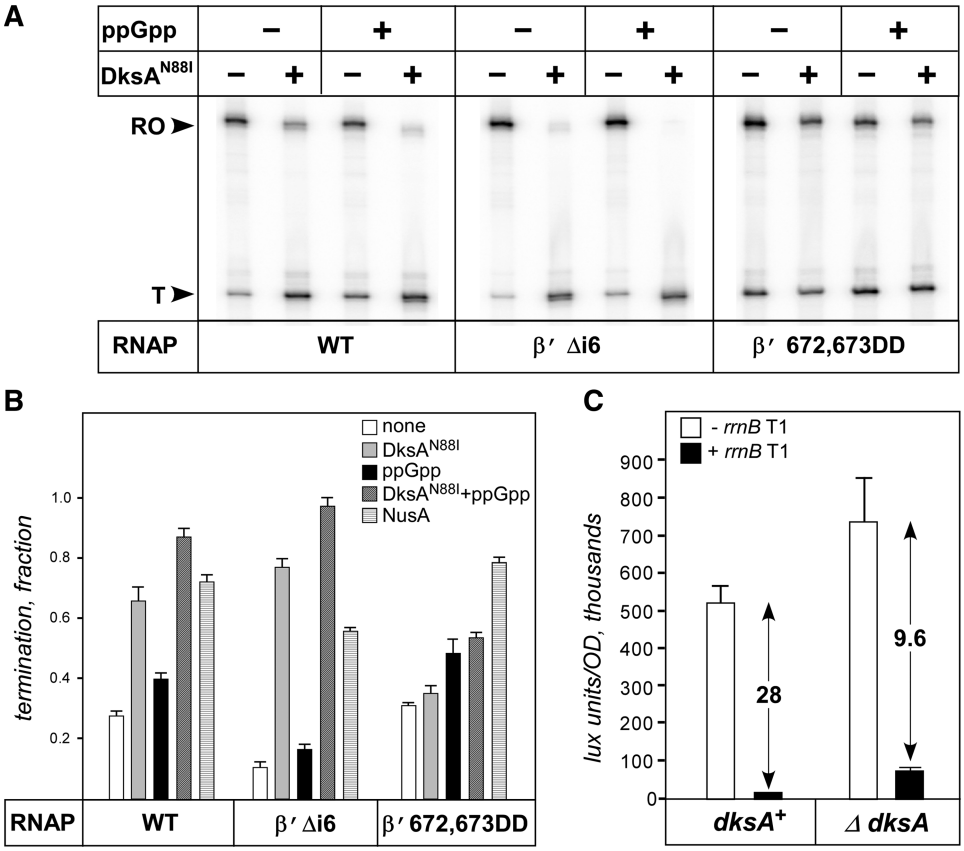

Figure 3. DksA increases efficiency of the *rrnB* T1 terminator. (**A**) Single-round transcription assays on pIA1088 template encoding a minimal *rrnB* T1 signal. Halted C105 complexes were formed on linear pIA1088 template (30 nM) with holo RNAP (40 nM, WT of mutant), ApU (100 μM) and starting NTPs (10 μM CTP, ATP and CTP, 10 μCi [α^{32}P]-CTP, 3000 Ci/mmol) in TGA14 (same as TGA2 but with 14 mM Mg-acetate) for 15 min at 37°C. DksA^{N88I} (2 μM) and ppGpp (30 μM) were added for 3 min at 37°C. Elongation was restarted by the addition of 250 μM NTPs and 10 μg/ml heparin. Reactions were quenched after 10-min incubation at 37°C and analyzed on 6% denaturing gels; a representative gel is shown, with the position of the terminated RNA (T, 155 nt) and run-off RNA (RO, 227 nt) indicated. (**B**) Termination efficiency was measured from three independent experiments; the data are presented as average ± standard deviation. For comparison, the effect of NusA (2 μM) has also been determined. (**C**) The expression of *lux* operon was measured with reporters containing or lacking the *rrnB* T1 terminator downstream from a T7A1 promoter in *dksA*+ and *dksA::tet* strains (CH458 and CH2294, a gift from Christophe Herman), as described in ref. 44. The results are expressed as luminescence corrected for the cell densities of individual cultures (in the range of OD_{600} = 1.8–2.0) divided by a factor of 1000. The lowest value was 100 times larger than the detection limit. The data represent the average ± standard deviation of three independent experiments.

37°C in the presence of 10 mM Mn^{2+}, the C27 RNA was rapidly degraded. DksA^{N88I} did not have any effect, whereas ppGpp slightly reduced the rate of cleavage. However, when both DksA and ppGpp were added, RNA cleavage was almost completely blocked. These observations are consistent with our earlier report that ppGpp/DksA compete with tagetitoxin, which strongly inhibits the exonuclease activity (12).

We next tested DksA effect on RNA cleavage in halted radiolabeled A26 ECs which are prone to backtracking and are thus very susceptible to GreB (11). We found that neither DksA^{N88I} nor ppGpp changed the kinetics of A26 RNA cleavage (Figure 5B). No effect on RNA cleavage was observed with the WT DksA present at concentrations up to 30 μM (IA, data not shown) even after an hour-long incubation. In contrast, A26 RNA was rapidly cleaved in the presence of 50 nM GreB (Supplementary Figure S8). Thus, DksA lacks the 'signature' activity of GreB, the RNA cleavage rate enhancement.

DksA does not affect the stalled EC

DksA alters RNAP interactions with the *rrnB* P1 promoter DNA in front of the active site: in the presence of DksA, DNaseI footprint is shortened at the downstream edge (8) and the initiation complex is destabilized. We wanted to test whether DksA destabilizes ECs and alters their structures.

First, we carried out DNaseI footprinting on an EC halted by nucleotide deprivation at position 147 on pRL596 template. In the EC, positions from −14 to +15 (relative to the active site) are protected against DNaseI cleavage (Figure 6A), consistent with the results obtained under the same conditions with other defined ECs (24). In contrast to the effects observed with *rrnB* P1 promoter complexes, we did not detect significant changes in protection upon addition of DksA^{N88I}, with or without ppGpp (Figure 6A and Supplementary Figure S8). Interestingly, effects of DksA are not always associated with an altered DNAseI protection, as observed at the

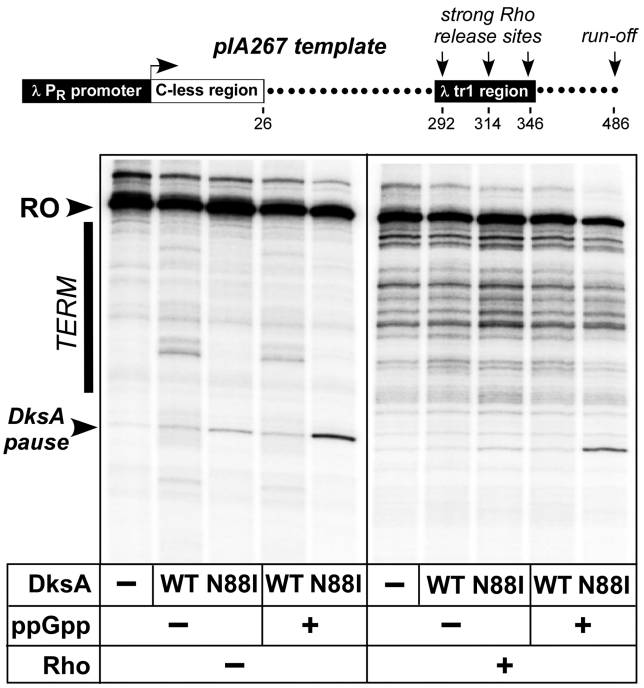

Figure 4. DksA does not affect Rho-dependent termination. Halted after addition of A26 on pIA267 template (shown on top) ECs were prepared at 50 nM in the absence of CTP in 30 µl of Rho buffer (40 mM Tris–HCl, 50 mM KCl, 5 mM $MgCl_2$, 0.1 mM dithiothreitol, 3% glycerol, pH 7.9) supplemented with ApU at 150 µM, ATP and UTP at 2.5 µM, GTP at 1 µM, and 5 µCi of [α^{32}P]GTP (3000 Ci/mmol) during 15 min incubation at 37°C. DksA variants were added to 2.5 µM, ppGpp – to 25 µM where indicated, followed by 3 min incubation at 37°C. Transcription was restarted by addition of NTPs to 25 µM and rifapentin to 20 µg/ml. Reactions were incubated at 37°C for 15 min and separated on 5% denaturing gels. Positions of the run-off (RO) transcript and the DksA-induced pauses are shown by arrows; position of the Rho-dependent termination region is indicated by a bar. The assay was repeated at least three times for each combination of factors; the differences between independent measurements were within 10%.

T7A1 (Supplementary Figure S3) and the λP_R promoters (23).

We next assayed DksA effect on EC stability. The ECs are very stable under most *in vitro* conditions, necessitating the use of destabilizing solutes (e.g. 1 M KCl, 50 mM EDTA, etc.) or release factors to observe their dissociation. Since DksA activity is reduced at KCl concentrations above 300 mM, we used *E. coli* Mfd, which releases RNAPs stalled at sites of DNA damage (24), to destabilize the EC instead. Because the Mfd-binding site on RNAP is located ~80 Å away from the RH (10), we reasoned that the two proteins would not compete. We assayed the effect of DksA on Mfd-mediated release of RNA from stalled EC immobilized on streptavidin beads via a biotin tag on the DNA template. We found that $DksA^{N88I}$ (at 5 µM) and ppGpp (at 100 µM) accelerated G37 EC dissociation in the presence of Mfd by <2-fold (Figure 6B); no effect was observed at four other halted ECs. These results indicate that DksA does not bind to static ECs or does not alter their structure.

DISCUSSION

Here, we report that DksA has many effects on transcript elongation, which are amplified by ppGpp, N88I substitution in DksA, and the β′i6 deletion and abolished by substitutions in the β′RH. However, DksA has no effect on RNA cleavage in arrested ECs. In contrast, Gre factors, which also bind to the β′RH, are not known to affect termination, are unable to modify RNAP lacking i6, and induce strong endonucleolytic cleavage of the nascent RNA in arrested ECs. We argue that the interplay among diverse regulators binding within the secondary channel should be viewed as differential targeting rather than competition, and is controlled by the conformational state of the EC that each protein recognizes.

Competition and redundancy among the secondary channel regulators

DksA inhibits transcription from *rrn* promoters (1) and enables ppGpp to act in the absence of the ω subunit of RNAP (25). DksA also activates amino acid biosynthesis promoters (7). GreB can substitute for DksA in destabilizing *rrnB* P1 promoter complexes but cannot mediate positive control or obviate the need for ω (14). In contrast, GreA does not inhibit (14) and may even activate (26) *rrnB* P1 promoter.

In the cell, DksA is far more abundant than GreB and has higher affinity than GreA for free RNAP (14). Although Gre factors can act similarly (14) or antagonistically (26) to DksA when overexpressed, the cellular conditions that lead to high levels of Gre factors are not known and DksA is expected to dominate the effect on initiation. However, this raises the question of how competition between Gre factors and DksA is avoided during elongation. We show that DksA and GreB elongation effects are non-overlapping, at least *in vitro*. Most importantly, DksA lacks the key activity of GreB, reactivation of backtracked ECs, which contributes to error correction (27). Thus, GreB and DksA likely target different ECs (Figure 7).

Many states of the transcription complexes

Regrettably, we do not know what these targets are for most factors that recognize a particular RNAP state rather than a DNA or RNA sequence. During initiation, several complexes that differ in interactions with the nucleic acids and conformations of RNAP domains co-exist and interconvert even at the same promoter, and distribution among these complexes is promoter specific (28). Depending on a promoter, DksA can repress, activate, or have no effect on initiation, and its effects are correlated with the promoter complex structure (29).

The ECs also exist in a variety of states which have been captured in structures and inferred from solution experiments. These states differ in the position of the RNA 3′ end, conformations of the TL, the state of the clamp, etc.; reviewed in ref. (30). Zenkin and colleagues (31) argued that *Thermus aquaticus* Gre does not act upon the active ECs and specifically targets backtracked complexes. Yokoyama and colleagues (5) reported a structure of

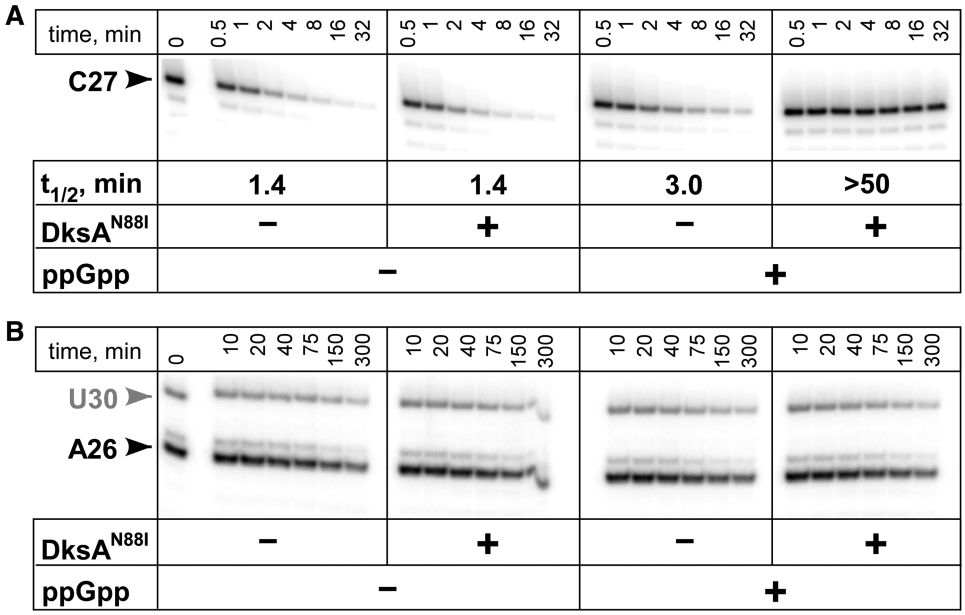

Figure 5. DksA effects on exo- (**A**) and endo- (**B**) RNA cleavage in halted ECs. DksA^{N88I} (10 μM) and ppGpp (100 μM) were added where indicated. Cleavage reactions were quenched at the indicated times and analyzed on a 10% gel. The assay was repeated at least three times for each combination of factors.

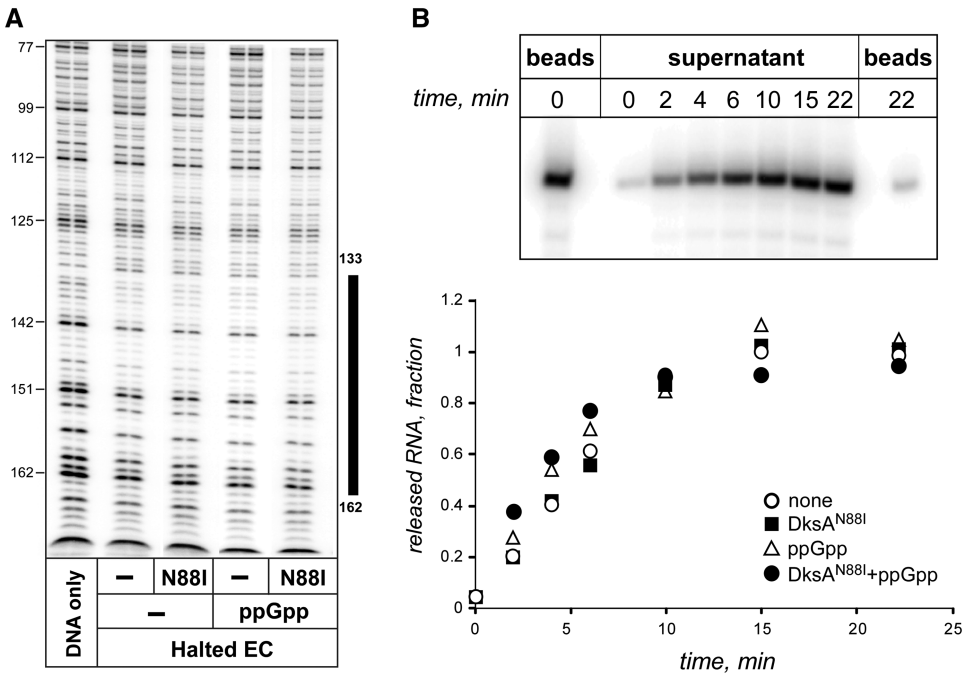

Figure 6. DksA does not affect the structure or stability of the halted EC. (**A**) DNaseI footprint boundaries of the C147 EC (indicated by a black bar on the right) were determined using a dideoxy sequencing ladder generated with the same labeled primer; numbers on the left mark positions from the transcription start site. The pattern of protection did not change when DksA and ppGpp were present, as indicated below each panel; the traces are shown in Supplementary Figure S8. (**B**) Mfd-mediated dissociation of the G37 EC immobilized on streptavidin-coated DynaBeads T1 (Invitrogen) in TGA10 with 200 mM NaCl. ^{32}P-labeled G37 ECs were mixed with Mfd (200 nM), DksA^{N88I} (5 μM) and ppGpp (100 μM) were added as indicated, and the complexes were incubated at 37°C for 2 min. Reactions were initiated by addition of 5 mM ATP, the released (into the supernatant) RNA was removed at the indicated times and analyzed on a 10% denaturing gel (shown on top). The fractions of released G37 RNA were determined from three independent experiments for each combination of factors. The half-lives (in min) were: 5.9 ± 0.5 with RNAP alone, 5.4 ± 0.6 with 5 μM DksA^{N88I}, 3.8 ± 0.4 with 100 μM ppGpp and 3.6 ± 0.4 with both ppGpp and DksA^{N88I}.

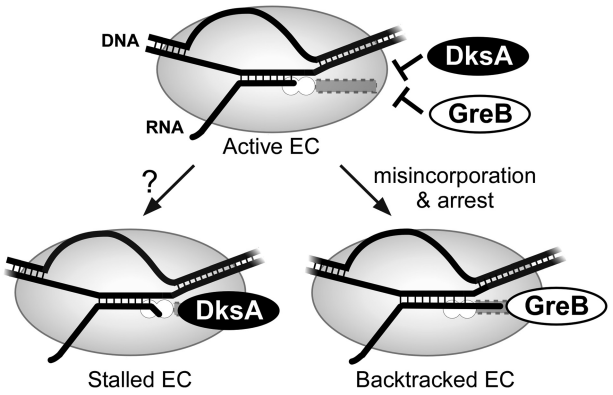

Figure 7. DksA and GreB target different ECs. Neither protein binds to an actively transcribing EC. GreB recognizes ECs that have backtracked, e.g. as a result of misincorporation, and cleaves the nascent RNA to restore its register in the active site (joined circles). DksA recognizes ECs that are stalled (shown with the 3' end of the RNA misaligned), e.g. during starvation, and rescues them by an unknown mechanism.

T. thermophilus EC bound to Gfh1. This structure and subsequent analysis suggest that Gfh1 (and Gre factors) stabilizes a very open, 'ratcheted' RNAP state.

Effects of TL on DksA and GreB

The TL appears to interact (positively or negatively) with all secondary channel ligands. The bacterial TL assumes many alternative states, from unfolded, invisible in the apo-enzyme structure, to a catalytic, α-helical hairpin folded state (trigger helices, THs) stabilized by binding of the substrate NTP (32). Binding of an inhibitor, such as streptolydigin (32,33) or tagetitoxin (34), or formation of an off-pathway intermediate (35) traps the TL in one of many alternative inactive states.

Our data suggest that DksA and GreB prefer different states of the TL. The folded TH state is incompatible with binding of Gre and Gfh1 factors (5), and the entire TL is dispensable for Gre activity (31). Removal of i6 makes *E. coli* RNAP resistant to GreB (17). Since many bacteria contain GreB but not i6, these effects support a model in which i6 acts indirectly, by altering the TL conformation; Δi6 RNAP is also resistant to pausing, which involves rearrangements of the TL (35).

In contrast, DksA activity, but not binding, is dependent on the TL (Figure 1 and ref. 8) and Δi6 strongly enhances DksA effects on elongation (Figures 2 and 3). A part of this effect could be due to stabilization of a TL conformation required for DksA action. The TH state may be incompatible with DksA binding in the secondary channel, but DksA may establish productive contacts with some other state of the TL. Signal transduction via the TL could explain effects of DksA on catalysis (this work) and its communication with distant switches (8). Differential responses of RNAP with 'fast' and 'slow' substitutions to DksA (Supplementary Figure S9) and synergy between ppGpp and DksA could be explained if ppGpp and fast RNAPs favors the RNAP conformation that is recognized by DksA.

We failed to identify an EC that responds to DksA from a collection of complexes halted by nucleotide deprivation. This suggests that DksA targets a state that is transiently populated during elongation. This is reminiscent of the DksA effects on initiation complexes: although DksA has been shown to alter transcription at different promoters, the *rrnB* P1, which does not form stable open complexes in the absence of NTP substrates, remains the only promoter at which DksA visibly changes the RNAP/DNA contacts (8).

DksA and DNA repair

Recent data indicate that ppGpp and DksA may play important roles at the interface of transcription and DNA repair by helping to remove RNAPs stalled at the site of DNA damage (36,37). McGlynn and Lloyd (38) showed that an increase in ppGpp synthesis or *rpo** substitutions in RNAP, a subset of stringent (ppGpp-mimicking) mutations, alleviate UV-sensitivity of strains lacking RuvABC. This led to a hypothesis that ppGpp and *rpo** substitutions, many of which likely compromise RNAP interactions with the nucleic acids, destabilize the stalled EC thereby facilitating repair and subsequent replication (38,39).

Soon after the role DksA as a ppGpp cofactor was discovered, the Lloyd lab showed that DksA, along with Mfd and GreA, is also necessary for UV-resistance and viability of strains in which repair is defective (37). Wang and co-authors demonstrated that DksA and Gre proteins prevented arrest of DNA replication during nutrient stress (36); their results argue that DksA acts upon the stalled ECs. These studies, together with a recent report that Rho guards *E. coli* against double-stranded breaks (40), reveal that (at least) four very different regulators could remove the inactivated ECs: DksA/ppGpp, Rho, Mfd and GreA. Interestingly, the same RNAP substitution, *rpo*35* (βH1244Q), suppresses defects in Rho function (40), *mfd* and *greA greB* phenotypes (39), and sensitivity to mitomycin C conferred by the *dksA* deletion (37), consistent with a common origin of these defects.

Why do bacteria need several, possibly redundant, mechanisms to remove stalled RNAPs? This redundancy may ensure that all transcription/replication collisions are resolved; indeed, simultaneous removal of any two factors exacerbates repair defects (37). Another reason may be that, although some of these factors display overlapping activities *in vitro* and even *in vivo*, their natural targets may be somewhat different. For example, although both Mfd and DksA enable survival of *ruv* strains (37), only DksA relieves starvation-induced replication arrest (36).

Most transcription elongation factors do not recognize specific sequences but display some preferences for the EC structure. Rho targets paused but not backtracked RNAPs (41). Gre factors rescue backtracked ECs (3) and do not bind to active ECs (31). Mfd recruits the nucleotide excision repair proteins to a DNA lesion after removing the RNAP stalled at the site of damage (42); thus, stalled enzymes are likely backtracked and Mfd can reactivate backtracked ECs *in vitro* (43). DksA target is yet unknown. A combination of structural,

biochemical and genome-wide analyses will be required to reveal the molecular mechanism by which DksA and other transcription factors identify their targets.

SUPPLEMENTARY DATA

Supplementary Data are available at NAR Online: Supplementary Table 1, Supplementary Figures 1–10 and Supplementary References [45–51].

ACKNOWLEDGEMENTS

We thank Rick Gourse, Chris Lennon, Wilma Ross, and Oleg Tsodikov for comments on the manuscript, and Georgiy Belogurov and Ruth Saecker for stimulating discussions.

FUNDING

The National Institutes of Health (GM67153) and the National Science Foundation (MCB-0949569). Funding for open access charge: the National Science Foundation (MCB-0949569).

Conflict of interest statement. None declared.

REFERENCES

1. Paul,B.J., Barker,M.M., Ross,W., Schneider,D.A., Webb,C., Foster,J.W. and Gourse,R.L. (2004) DksA: a critical component of the transcription initiation machinery that potentiates the regulation of rRNA promoters by ppGpp and the initiating NTP. *Cell*, **118**, 311–322.
2. Potrykus,K. and Cashel,M. (2008) (p)ppGpp: still magical? *Annu. Rev. Microbiol.*, **62**, 35–51.
3. Laptenko,O., Lee,J., Lomakin,I. and Borukhov,S. (2003) Transcript cleavage factors GreA and GreB act as transient catalytic components of RNA polymerase. *EMBO J.*, **22**, 6322–6334.
4. Perederina,A., Svetlov,V., Vassylyeva,M.N., Tahirov,T.H., Yokoyama,S., Artsimovitch,I. and Vassylyev,D.G. (2004) Regulation through the secondary channel – structural framework for ppGpp-DksA synergism during transcription. *Cell*, **118**, 297–309.
5. Tagami,S., Sekine,S., Kumarevel,T., Hino,N., Murayama,Y., Kamegamori,S., Yamamoto,M., Sakamoto,K. and Yokoyama,S. (2010) Crystal structure of bacterial RNA polymerase bound with a transcription inhibitor protein. *Nature*, **468**, 978–982.
6. Sosunova,E., Sosunov,V., Kozlov,M., Nikiforov,V., Goldfarb,A. and Mustaev,A. (2003) Donation of catalytic residues to RNA polymerase active center by transcription factor Gre. *Proc. Natl Acad. Sci. USA*, **100**, 15469–15474.
7. Paul,B.J., Berkmen,M.B. and Gourse,R.L. (2005) DksA potentiates direct activation of amino acid promoters by ppGpp. *Proc. Natl Acad. Sci. USA*, **102**, 7823–7828.
8. Rutherford,S.T., Villers,C.L., Lee,J.H., Ross,W. and Gourse,R.L. (2009) Allosteric control of *Escherichia coli* rRNA promoter complexes by DksA. *Genes Dev.*, **23**, 236–248.
9. Blankschien,M.D., Lee,J.H., Grace,E.D., Lennon,C.W., Halliday,J.A., Ross,W., Gourse,R.L. and Herman,C. (2009) Super DksAs: substitutions in DksA enhancing its effects on transcription initiation. *EMBO J.*, **28**, 1720–1731.
10. Deaconescu,A.M., Chambers,A.L., Smith,A.J., Nickels,B.E., Hochschild,A., Savery,N.J. and Darst,S.A. (2006) Structural basis for bacterial transcription-coupled DNA repair. *Cell*, **124**, 507–520.
11. Vassylyeva,M.N., Svetlov,V., Dearborn,A.D., Klyuyev,S., Artsimovitch,I. and Vassylyev,D.G. (2007) The carboxy-terminal coiled-coil of the RNA polymerase beta′-subunit is the main binding site for Gre factors. *EMBO Rep.*, **8**, 1038–1043.
12. Vassylyev,D.G., Svetlov,V., Vassylyeva,M.N., Perederina,A., Igarashi,N., Matsugaki,N., Wakatsuki,S. and Artsimovitch,I. (2005) Structural basis for transcription inhibition by tagetitoxin. *Nat. Struct. Mol. Biol.*, **12**, 1086–1093.
13. Lennon,C.W., Gaal,T., Ross,W. and Gourse,R.L. (2009) *Escherichia coli* DksA binds to Free RNA polymerase with higher affinity than to RNA polymerase in an open complex. *J. Bacteriol.*, **191**, 5854–5858.
14. Rutherford,S.T., Lemke,J.J., Vrentas,C.E., Gaal,T., Ross,W. and Gourse,R.L. (2007) Effects of DksA, GreA, and GreB on transcription initiation: insights into the mechanisms of factors that bind in the secondary channel of RNA polymerase. *J. Mol. Biol.*, **366**, 1243–1257.
15. Artsimovitch,I., Svetlov,V., Murakami,K.S. and Landick,R. (2003) Co-overexpression of *Escherichia coli* RNA polymerase subunits allows isolation and analysis of mutant enzymes lacking lineage-specific sequence insertions. *J. Biol. Chem.*, **278**, 12344–12355.
16. Opalka,N., Brown,J., Lane,W.J., Twist,K.A., Landick,R., Asturias,F.J. and Darst,S.A. (2010) Complete structural model of *Escherichia coli* RNA polymerase from a hybrid approach. *PLoS Biol*, **8**, e1000483.
17. Zhang,J., Palangat,M. and Landick,R. (2009) Role of the RNA polymerase trigger loop in catalysis and pausing. *Nat. Struct. Mol. Biol.*, **17**, 99–104.
18. Kingston,R.E., Nierman,W.C. and Chamberlin,M.J. (1981) A direct effect of guanosine tetraphosphate on pausing of *Escherichia coli* RNA polymerase during RNA chain elongation. *J. Biol. Chem.*, **256**, 2787–2797.
19. Artsimovitch,I., Patlan,V., Sekine,S., Vassylyeva,M.N., Hosaka,T., Ochi,K., Yokoyama,S. and Vassylyev,D.G. (2004) Structural basis for transcription regulation by alarmone ppGpp. *Cell*, **117**, 299–310.
20. Krohn,M. and Wagner,R. (1996) Transcriptional pausing of RNA polymerase in the presence of guanosine tetraphosphate depends on the promoter and gene sequence. *J. Biol. Chem.*, **271**, 23884–23894.
21. Buckstein,M.H., He,J. and Rubin,H. (2008) Characterization of nucleotide pools as a function of physiological state in *Escherichia coli*. *J. Bacteriol.*, **190**, 718–726.
22. Lau,L.F. and Roberts,J.W. (1985) Rho-dependent transcription termination at lambda R1 requires upstream sequences. *J. Biol. Chem.*, **260**, 574–584.
23. Symersky,J., Perederina,A., Vassylyeva,M.N., Svetlov,V., Artsimovitch,I. and Vassylyev,D.G. (2006) Regulation through the RNA polymerase secondary channel. Structural and functional variability of the coiled-coil transcription factors. *J. Biol. Chem.*, **281**, 1309–1312.
24. Krummel,B. and Chamberlin,M.J. (1992) Structural analysis of ternary complexes of *Escherichia coli* RNA polymerase. Deoxyribonuclease I footprinting of defined complexes. *J. Mol. Biol.*, **225**, 239–250.
25. Vrentas,C.E., Gaal,T., Ross,W., Ebright,R.H. and Gourse,R.L. (2005) Response of RNA polymerase to ppGpp: requirement for the omega subunit and relief of this requirement by DksA. *Genes Dev.*, **19**, 2378–2387.
26. Potrykus,K., Vinella,D., Murphy,H., Szalewska-Palasz,A., D'Ari,R. and Cashel,M. (2006) Antagonistic regulation of *Escherichia coli* ribosomal RNA rrnB P1 promoter activity by GreA and DksA. *J. Biol. Chem.*, **281**, 15238–15248.
27. Zenkin,N., Yuzenkova,Y. and Severinov,K. (2006) Transcript-assisted transcriptional proofreading. *Science*, **313**, 518–520.
28. Saecker,R.M., Record,M.T. Jr and Dehaseth,P.L. (2011) Mechanism of bacterial transcription initiation: RNA polymerase - promoter binding, isomerization to initiation-competent open complexes, and initiation of RNA synthesis. *J. Mol. Biol.*, **412**, 754–771.

29. Haugen,S.P., Ross,W. and Gourse,R.L. (2008) Advances in bacterial promoter recognition and its control by factors that do not bind DNA. *Nat. Rev. Microbiol.*, **6**, 507–519.
30. Nudler,E. (2009) RNA polymerase active center: the molecular engine of transcription. *Annu. Rev. Biochem.*, **78**, 335–361.
31. Roghanian,M., Yuzenkova,Y. and Zenkin,N. (2011) Controlled interplay between trigger loop and Gre factor in the RNA polymerase active centre. *Nucleic Acids Res.*, **39**, 4352–4359.
32. Vassylyev,D.G., Vassylyeva,M.N., Zhang,J., Palangat,M., Artsimovitch,I. and Landick,R. (2007) Structural basis for substrate loading in bacterial RNA polymerase. *Nature*, **448**, 163–168.
33. Tuske,S., Sarafianos,S.G., Wang,X., Hudson,B., Sineva,E., Mukhopadhyay,J., Birktoft,J.J., Leroy,O., Ismail,S., Clark,A.D. Jr *et al.* (2005) Inhibition of bacterial RNA polymerase by streptolydigin: stabilization of a straight-bridge-helix active-center conformation. *Cell*, **122**, 541–552.
34. Artsimovitch,I., Svetlov,V., Nemetski,S.M., Epshtein,V., Cardozo,T. and Nudler,E. (2011) Tagetitoxin inactivates transcription inhibits RNA polymerase through trapping of the trigger loop. *J. Biol. Chem.*, **286**, 40395–40400.
35. Toulokhonov,I., Zhang,J., Palangat,M. and Landick,R. (2007) A central role of the RNA polymerase trigger loop in active-site rearrangement during transcriptional pausing. *Mol. Cell*, **27**, 406–419.
36. Tehranchi,A.K., Blankschien,M.D., Zhang,Y., Halliday,J.A., Srivatsan,A., Peng,J., Herman,C. and Wang,J.D. (2010) The transcription factor DksA prevents conflicts between DNA replication and transcription machinery. *Cell*, **141**, 595–605.
37. Trautinger,B.W., Jaktaji,R.P., Rusakova,E. and Lloyd,R.G. (2005) RNA polymerase modulators and DNA repair activities resolve conflicts between DNA replication and transcription. *Mol. Cell*, **19**, 247–258.
38. McGlynn,P. and Lloyd,R.G. (2000) Modulation of RNA polymerase by (p)ppGpp reveals a RecG-dependent mechanism for replication fork progression. *Cell*, **101**, 35–45.
39. Trautinger,B.W. and Lloyd,R.G. (2002) Modulation of DNA repair by mutations flanking the DNA channel through RNA polymerase. *EMBO J.*, **21**, 6944–6953.
40. Washburn,R.S. and Gottesman,M.E. (2011) Transcription termination maintains chromosome integrity. *Proc. Natl Acad. Sci. USA*, **108**, 792–797.
41. Dutta,D., Chalissery,J. and Sen,R. (2008) Transcription termination factor rho prefers catalytically active elongation complexes for releasing RNA. *J. Biol. Chem.*, **283**, 20243–20251.
42. Selby,C.P. and Sancar,A. (1993) Molecular mechanism of transcription-repair coupling. *Science*, **260**, 53–58.
43. Park,J.S. and Roberts,J.W. (2006) Role of DNA bubble rewinding in enzymatic transcription termination. *Proc. Natl Acad. Sci. USA*, **103**, 4870–4875.
44. Belogurov,G.A., Sevostyanova,A., Svetlov,V. and Artsimovitch,I. (2010) Functional regions of the N-terminal domain of the antiterminator RfaH. *Mol. Microbiol.*, **76**, 286–301.
45. Ederth,J., Artsimovitch,I., Isaksson,L.A. and Landick,R. (2002) The downstream DNA jaw of bacterial RNA polymerase facilitates both transcriptional initiation and pausing. *J. Biol. Chem.*, **277**, 37456–37463.
46. Artsimovitch,I. and Landick,R. (2000) Pausing by bacterial RNA polymerase is mediated by mechanistically distinct classes of signals. *Proc. Natl Acad. Sci. USA*, **97**, 7090–7095.
47. Artsimovitch,I., Svetlov,V., Anthony,L., Burgess,R.R. and Landick,R. (2000) RNA polymerases from *Bacillus subtilis* and *Escherichia coli* differ in recognition of regulatory signals *in vitro*. *J. Bacteriol.*, **182**, 6027–6035.
48. Feng,G.H., Lee,D.N., Wang,D., Chan,C.L. and Landick,R. (1994) GreA-induced transcript cleavage in transcription complexes containing *Escherichia coli* RNA polymerase is controlled by multiple factors, including nascent transcript location and structure. *J. Biol. Chem.*, **269**, 22282–22294.
49. Belogurov,G.A., Vassylyeva,M.N., Svetlov,V., Klyuyev,S., Grishin,N.V., Vassylyev,D.G. and Artsimovitch,I. (2007) Structural basis for converting a general transcription factor into an operon-specific virulence regulator. *Mol Cell*, **26**, 117–129.
50. Svetlov,V., Belogurov,G.A., Shabrova,E., Vassylyev,D.G. and Artsimovitch,I. (2007) Allosteric control of the RNA polymerase by the elongation factor RfaH. *Nucleic Acids Res.*, **35**, 5694–5705.
51. Artsimovitch,I. and Landick,R. (2002) The transcriptional regulator RfaH stimulates RNA chain synthesis after recruitment to elongation complexes by the exposed nontemplate DNA strand. *Cell*, **109**, 193–203.